

# Coherent diffraction patterns of individual dislocation strain fields

I K Robinson<sup>1</sup>, Y Da<sup>2</sup>, T Spila<sup>2</sup> and J E Greene<sup>2</sup>

<sup>1</sup> Department of Physics, University of Illinois, Urbana, USA

<sup>2</sup> Department of Materials Science and Engineering, University of Illinois, Urbana, USA

E-mail: ikr@uiuc.edu

Received 1 March 2005

Published

Online at [stacks.iop.org/JPhysD/38](http://stacks.iop.org/JPhysD/38)

## Abstract

The coherent x-ray diffraction (CXD) method is particularly attractive for understanding structures that can be represented as phase objects.

Diffraction from a crystal acquires a phase whenever atoms are displaced from lattice sites, even by small fractions of an Angstrom, so CXD measured around a Bragg peak is ideal for studying strain. We have succeeded in using these coherent beams to study the strain field arising from individual misfit dislocations located at an interface between a GeSi thin film and its Si(001) substrate. The data have not yet been inverted to images, but we show how the asymmetric CXD diffraction patterns can be explained qualitatively by a model phase structure.

AQ1 (Some figures in this article are in colour only in the electronic version)

## 1. Introduction

Gas-source molecular beam epitaxy (GSMBE) is a form of chemical vapour deposition (CVD) growth technique for semiconductors that allows the preparation of semiconductor thin films of exquisitely high quality. The investigation of the structure of epitaxial thin films, starting with those prepared by MBE or CVD, allowed exploration of the principles of critical film thickness to be tested quantitatively [1]. X-ray diffraction analysis was a significant contribution to this early confirmation of the concept of critical thickness, as introduced by Matthews and Blakeslee [2].

The structure of crystal defects is one of the fundamental scientific questions underlying materials science. Most previous work has been achieved by lattice-imaging electron microscopy, but these methods suffer from invasive sample preparation artefacts that can disrupt the structures. Dislocations, one of the most important crystal defects, are characteristic topological line defects in a crystal lattice in which the lattice fails to repeat around the defect line, missing by a displacement called the Burgers vector. Thin films of dissimilar materials of different lattice parameter will have misfit, which can be accommodated by an array of edge dislocations at the interface, each responsible for one lattice unit of misfit. The inserted or deleted planes that end at the edge dislocation then glide through the lattice of the

thin film along a slip plane that emerges eventually from the surface.

The dislocation and slip plane structures are decorated with a strain field that decays in amplitude with distance from the structure in the lattice. X-ray diffraction from such a structure sees interference between waves scattered by the displaced atoms, which is then phase-shifted with respect to the parent lattice. An image of the crystal obtained by inversion of diffraction data surrounding one of the Bragg peaks will acquire a phase which corresponds to the scalar product of the strain vector with the momentum transfer vector of the Bragg peak [3]. It is important to realize that atomic resolution is not required for the strain field to be visible because it extends over many lattice spacings. Imaging these individual characteristic strain fields to understand the strain relaxation mechanisms is the eventual goal of these studies.

The inversion methods (e.g. hybrid input–output) needed to obtain images are still under development, particularly for the case of complex images, such as those discussed here. In this paper, we report that the necessary diffraction patterns can be obtained and show our progress to date in being able to model the asymmetric patterns that result. In our experiments, we prepared a micrometre-sized coherent beam of x-rays using Kirkpatrick–Baez (KB) optics and used it to measure diffraction from arrays of these dislocation structures in a Ge<sub>0.3</sub>Si<sub>0.7</sub> thin film. As the beam was scanned across the sample, the diffraction pattern changed

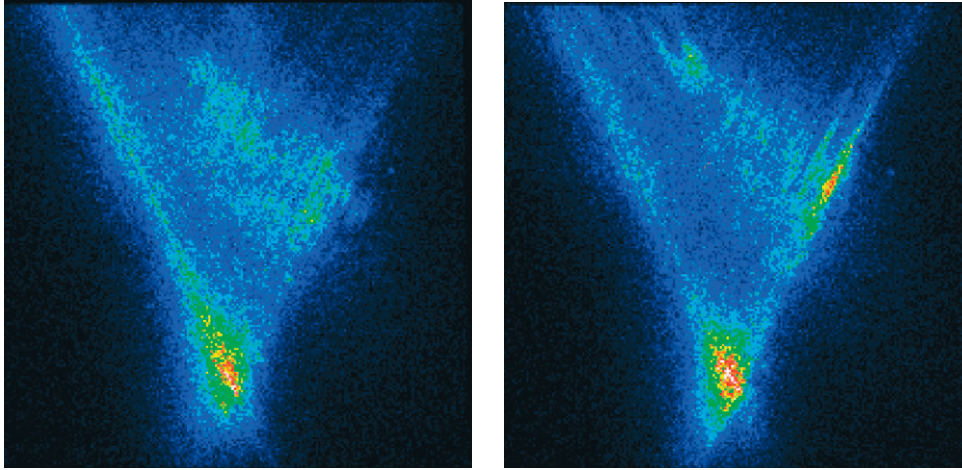


**Figure 1.** Measured coherent diffraction pattern of the 2800 Å film of  $\text{Ge}_{0.3}\text{Si}_{0.7}$  in the vicinity of its 202 Bragg peak. The pattern is a reciprocal lattice map centred on the bright spot at the bottom, which is the CTR position, indexing at reciprocal lattice coordinate  $(2, 0, 1.92)$ . The pattern is indexed in the Si coordinate system, with the  $(0, 0.55, 1)$  direction running up the page and  $(1, 0, 0)$  to the right. The sample was shifted sideways by a few micrometres in between the two pictures.

significantly as individual dislocation structures entered and left the illuminated area.

## 2. Experimental methods

The sample used for these measurements was a film of  $\text{Ge}_{0.3}\text{Si}_{0.7}$  grown by GSMBE from  $\text{Ge}_2\text{H}_6/\text{Si}_2\text{H}_6$  mixtures at  $450^\circ\text{C}$ . It was grown on a Si(100) substrate to a thickness of 2800 Å slightly beyond the critical thickness. The critical thickness is the point of onset of the creation of interfacial dislocations, which can be detected as cusp-shaped ridges by atomic force microscopy (AFM) when they glide to the surface of the film along  $\{111\}$  planes [4]. The dislocations form a quadrangular array seen in the AFM with spacings in the micron range. The coherent x-ray diffraction (CXD) method is highly sensitive to the strain fields of these features.

The measurements were made at beamline 34-ID-C of the advanced photon source (APS). The sample was aligned by means of its Si(100) substrate then measured with a coherent beam of  $50 \times 50 \mu\text{m}^2$  focused down to about  $1 \times 1 \mu\text{m}^2$  using KB mirror optics following the coherence-defining aperture. The incidence angle of the beam onto the sample was fixed at  $1^\circ$ . The resulting diffraction pattern associated with the  $\text{Ge}_{0.3}\text{Si}_{0.7}$  film was measured with a direct detection charge-coupled device (CCD) x-ray camera placed 1.0 m away from the sample. The  $20 \mu\text{m}$  pixels were read out in a  $4 \times 4$  binning mode. The exposure time was typically 10 s. The sample position was scanned across the beam in steps of  $0.2 \mu\text{m}$  so that a sequence of frames was recorded as a function of position of the sample in the form of a movie.

The indexing of the features seen in the CCD employed a novel, but intuitive, method. After the sample is aligned correctly, the diffractometer control programme ('super') can centre an arbitrarily selected point of reciprocal space somewhere near the middle of the alignment slits, usually  $5 \times 5 \text{mm}^2$ . After the alignment detector is replaced by the CCD, the slits are opened to the full  $20 \times 20 \text{mm}^2$  field of view. The central feature on the CCD is then the calibrated point. Other features can be indexed by manual updates of the vertical and horizontal detector angles to bring them to

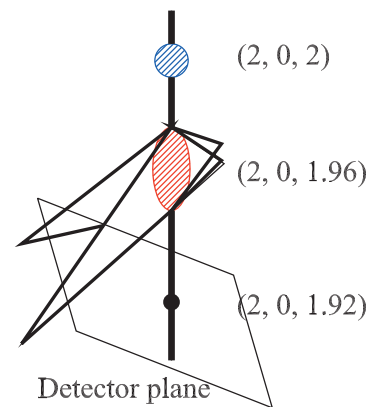


**Figure 2.** Sketch of the diffraction features referred to in this paper laid out in three dimensions. The substrate  $(2, 0, 2)$  and GeSi film  $(2, 0, 1.96)$  Bragg peaks are joined by a common vertical line which is the CTR of the (001) film surface. The triangular flares are the  $\{111\}$ -oriented CTRs of the glide planes in the structure, which emanate from the GeSi  $(2, 0, 1.96)$  Bragg peak. The CCD detector plane is tangent to the Ewald sphere passing through the measurement point  $(2, 0, 1.92)$  on the CTR. Two of the flares intersect the sphere at the diagonal locations, as observed.

the same centre position of the readout. The new detector angles are then converted back to reciprocal space by the diffractometer control programme.

## 3. Interpretation of diffraction pattern

Figure 1 shows two diffraction patterns from adjacent regions of this sample separated by a few micrometres. The bright spot at the bottom, which indexes at  $(2, 0, 1.92)$ , is the crystal truncation rod (CTR) [5] of the main GeSi Bragg peak at  $(2, 0, 1.96)$ , which is itself displaced from the (202) Si substrate peak because of tetragonal strain in the film. The two distinct diagonal features index as different combinations of  $\{111\}$  displacements from  $(2, 0, 1.96)$ . The crystal directions, derived using the method earlier, are indicated in the caption. The structure that causes them must resemble an extended planar defect in order to generate such a sharp feature, which

is reminiscent of a CTR [5]. The features are broad along the diagonal direction, suggesting they arise from objects that have the depth of the thin film. This is all consistent with attributing them to the  $\{111\}$  glide planes from the dislocations. The three-dimensional arrangement of this interpretation of these various features is sketched in figure 2.

However, as the small probe is scanned across the surface of the film, at different locations it encounters different distributions of dislocation structures. Since the dislocation array is coherently illuminated, the dislocation strain fields interfere with each other to fill up the triangle with fringes, as observed in figure 1. Comparison between the panels shows that, while the diagonal borders of the triangle are relatively conserved, the fringes redistribute dramatically as a function of position on the sample. When these diffraction patterns are eventually inverted, we expect we will see an image of the spatial distribution of dislocations in the film. In the meantime, we attempt to explain their origin by means of simulation.

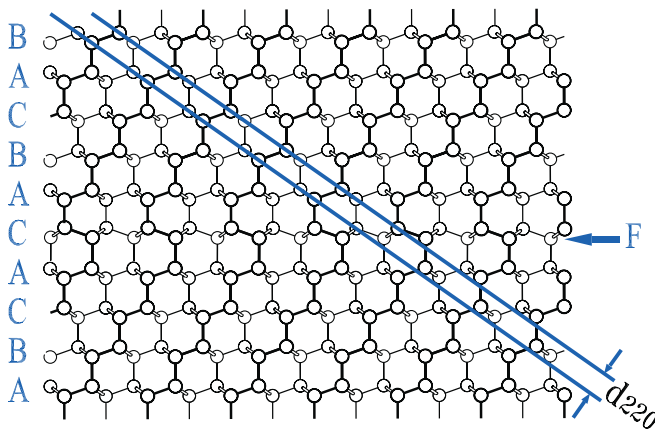


**Figure 3.** Illustration of a ‘deformation fault’ in the diamond lattice of silicon. Atoms in two planes are indicated by thick and thin lines with ‘ball and stick’ bonds. The labels ‘A’, ‘B’ and ‘C’ refer to the conventional ‘ABC’ sequence of  $\{111\}$  planes of the face-centred cubic lattice running up the page. When one ‘B’ double-layer is deleted, at the location indicated by the symbol ‘F’, the bonds still connect without any distortion. This deformation fault is, therefore, energetically favourable in silicon or GeSi.

It is worth noting that the diffraction patterns of figure 1 are highly asymmetric. In our earlier work on CXD from small crystals, patterns that were largely symmetric about the centre of the Bragg peak were observed [6]. This was attributed to the absence of strain in the nanocrystals used. The asymmetry of the diffraction patterns seen here must result from Fourier transformation of a complex, rather than real, density function and we have shown previously that strain in crystals can give rise to this situation [3].

#### 4. Modelling of the intensity distribution

This behaviour can be modelled by considering the dislocations to be phase structures that are associated with the  $\{111\}$  glide planes. Since GeSi has a larger lattice constant than Si, each slip structure will correspond to a  $\{111\}$  double layer missing from the lattice. This structure, called a ‘deformation fault’ is illustrated in figure 3. It can be seen directly how the deformation fault gives rise to a modification of the phase of diffraction from a set of  $\{220\}$  planes by drawing guide lines for those planes on the picture as shown. The atomic planes are aligned with the  $\{220\}$  guide lines on one side of the fault and are shifted by  $2\pi/3$  of a spacing on the other side. In the image obtained from inversion of diffraction around the  $(220)$  Bragg peak, the phase of the material on one side is, therefore, shifted by  $2\pi/3$  relative to the other.

This phase shift of  $2\pi/3$  is relaxed by the strain fields to bring the two sides of the plane back into commensuration with the Si(001) substrate. The  $\{111\}$  glide planes are inclined to the surface, which causes the phase shift to be spread sideways by a lateral distance of  $2000 \text{ \AA}$  over the  $2800 \text{ \AA}$  film thickness. Even though the total real-space amplitude is strictly not quite the same as the average of the phase, this can be considered to change linearly by  $2\pi$  over this  $2000 \text{ \AA}$  width. The direction of this average phase change does not depend on the tilt direction of the glide plane; because the GeSi film is under compression, this phase ramp always has the same sign.

We, therefore, model the experiment as a finite sized block of material of uniform density, but in which the phase is allowed to ramp from  $0$  to  $2\pi$  over a narrow band representing each

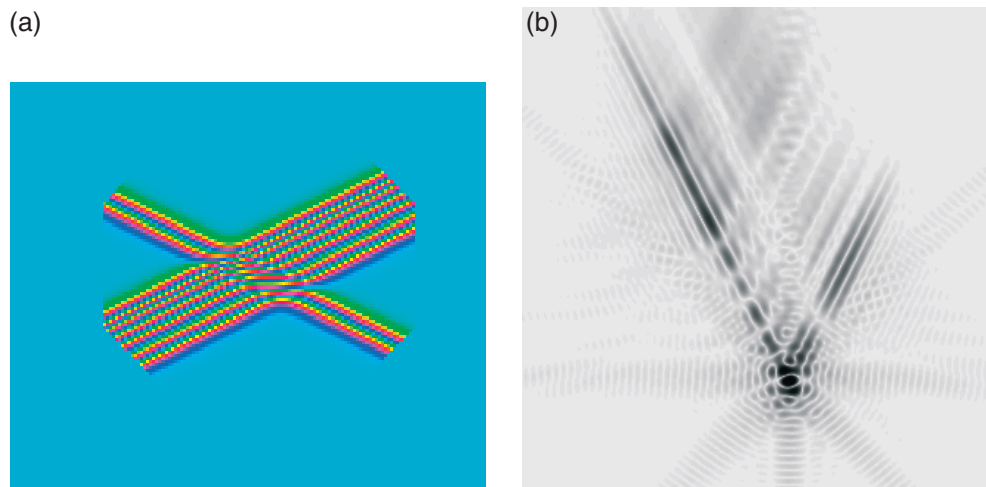


**Figure 4.** (a) Real-space model of the diffracting sample consisting of uniform amplitude (electron density) within a finite illuminated region and a real-space phase that varies across bands that represent the dislocations and their associated slip planes. (b) Fourier transform of this structure, which resembles the diffraction patterns seen in the experiment.

dislocation structure, including the slip plane. The reason the phase has to change by  $2\pi$  is that the GeSi thin film remains always in registry with the substrate far away from each dislocation. Figure 4 shows a two-dimensional array of these phase steps placed randomly, but with the phase always rising along the same two directions, as appropriate for our case of misfit of GeSi with Si. The direction (sign) of the phase step is independent of whether the dislocation glides to the left or to the right; it just depends on the sign of the misfit. The coloured stripes indicate the assumed spatial variation of the phase, following a colour wheel.

The amplitude of the diffraction pattern is obtained directly by Fourier transformation of the complex structure, using an FFT, and is plotted in figure 4(b). It is striking how well the general features of the data are reproduced, including the intermodulation of the two sets of fringes. The directions, density and width of the dislocation structures had been chosen to yield a diffracted intensity that is modulated in a way that resembles the diffraction patterns observed in the experiment. The pattern is also notable for its lack of centrosymmetry, as expected for a structure that has a significant influence of strain.

### Acknowledgments

This work was supported by the NSF under grant DMR 03-08660. The 34-ID-C CXD facility was built with funds

from NSF DMR 97-24294 and operated by UNICAT. The UNICAT facility at APS is supported by the University of Illinois Materials Research Laboratory, funded by the US Department of Energy (DOE) under DEFG02-91ER45439, Oak Ridge National Laboratory, the National Institute of Standards and Technologies and UOP Research & Development. The APS is itself supported by the DOE under contract No W 31 109 ENG 38.

### References

- [1] Fiory A T, Bean J C, Feldman L C and Robinson I K 1984 Commensurate and incommensurate structures in molecular beam epitaxially grown  $\text{Ge}_x\text{Si}_{1-x}$  films on Si(100) *J. Appl. Phys.* **56** 1227
- [2] Matthews J W and Blakeslee A E 1975 *J. Cryst. Growth* **29** 273
- [3] Robinson I K and Vartanyants I A 2001 Use of coherent x-ray diffraction to map strain fields in nanocrystals *Appl. Surf. Sci.* **182** 186–91
- [4] Spila T, Desjardins P, D’Arcy-Gall J, Twesten R D and Greene J E 2003 Effect of steady-state hydrogen coverage on the evolution of crosshatch morphology during  $\text{Si}_{1-x}\text{Ge}_x/\text{Si}(001)$  growth from hydride precursors *J. Appl. Phys.* **93** 1918–25
- [5] Robinson I K 1986 Crystal truncation rods and surface roughness *Phys. Rev. B* **33** 3830
- [6] Williams G J, Pfeifer M A, Vartanyants I A and Robinson I K 2003 Three-dimensional imaging of microstructure in gold nanocrystals *Phys. Rev. Lett.* **90** 175501-1

## **QUERIES**

### **Page 1**

AQ1

Please be aware that the colour figures in this article will only appear in colour in the web version. If you require colour in the printed journal and have not previously arranged it, please contact the production editor now.